Investigation of fatigue crack propagation in nickel superalloy using Diffraction contrast tomography and Phase Contrast tomography

Olivier M. D. M. Messé, Joël Lachambre, Andrew King, Jean-Yves Buffiere, Cathie M. F. Rae

Investigation of fatigue crack propagation in nickel superalloy using Diffraction contrast tomography and Phase Contrast tomography

O.M.D.M. Messé[1,a], J. Lachambre[2,b], A. King[3,c], J-Y Buffière[2,d] and C.M.F. Rae[1,e]

[1] Rolls-Royce UTC, Department of Materials Science & Metallurgy, University of Cambridge, 27 Charles Babbage Road, Cambridge CB3 0FS, UK

[2] MATEIS, Batiment B. Pascal, 5ème étage, 7 Avenue Jean Capelle, 69621 Villeurbanne, France

[3] Synchrotron SOLEIL, L'Orme des Merisiers Saint-Aubin, 91192 GIF-sur-YVETTE

[a] omdmm2@cam.ac.uk, [b] joel.lachambre@insa-lyon.fr, [c] king@synchrotron-soleil.fr, [d] jean-yves.buffiere@insa-lyon.fr, [e] cr18@cam.ac.uk

Keywords: Nickel superalloy, fatigue, crack propagation, tomography, image processing

Abstract.

Evaluation of superalloy component life in turbine engines requires a detailed understanding of how fatigue crack initiation and short crack propagation contribute to fatigue life. However most investigations have been carried out post-mortem and in two dimensions. New techniques are able to fully resolve cracks propagating in four dimensions (space and time), enabling characterisation of their local environments and allowing a much deeper understanding of fatigue mechanics.

Nickel-based superalloys experiencing high cycle fatigue have shown a high sensitivity to microstructure during initiation and short crack propagation. Using high energy X-rays and the combination of Diffraction Contrast Tomography (DCT) and Phase Contrast Tomography (PCT), we followed a fatigue crack initiated from a Focused Ion Beam (FIB) milled notch at room temperature. Analyses have been carried out to fully characterise the crack and its environment. We tracked the evolution of the crack and interactions with the microstructure. Subsequently, post-mortem investigations have been carried out to corroborate results obtained from the tomographs and to provide more local information of fatigue crack propagation.

Introduction

Nickel base superalloys form an important class of alloys that find widespread use in high integrity aeroengine applications and a detailed understanding of their degradation processes is critical to reliable estimates of component life. Recent studies of nickel base superalloys have identified the importance of microstructural features, such as twin boundaries, gamma prime (γ') size distribution in determining fatigue crack initiation and propagation [1-3]. The development of novel investigation techniques has granted new insights into already well-studied problems. Until recently, experimental investigations on fatigue were restricted to either post-mortem analysis of the crack shape and propagation in two dimensions. Tomography techniques combining diffraction and phase contrast tomography (DCT and PCT) give us a very powerful tool enabling the simultaneous investigation of the propagating crack and its interaction with the microstructure.

Experimental procedure

Sample Preparation

The material investigated in this study is a nickel base superalloy, RR1000, developed by Rolls-Royce plc. [4]. The material was processed via the powder metallurgy route, HIPped and forged. To facilitate grain reconstruction, the sample underwent a heat-treatment above the γ' supersolvus (1170°C) for 5 hours to allow grain growth and was air cooled to produce two populations of γ' precipitates (secondary and tertiary). Powder processing gives a fine distribution of (Ti,Ta)C at

prior particle boundaries however after heat treatment most are located within the grains. Due to the alloy processing and the low stacking fault energy, the specimen possesses a high density of twins.

Dog-bone specimens were cut from the heat-treated block using EDM, and were mechanically polished to give a 75µm square gauge length. To release the surface stresses from the EDM, cutting and polishing processes and produce rounded edges (to avoid stress concentration at the edges during fatigue), the specimens were electropolished using 7%vol perchloric acid in methanol at 0°C and 4 V. Finally, a notch (100×15×4µm) was FIB milled in the middle of the gauge length to initiate the crack using FEI Helios Dual Beam Microscope.

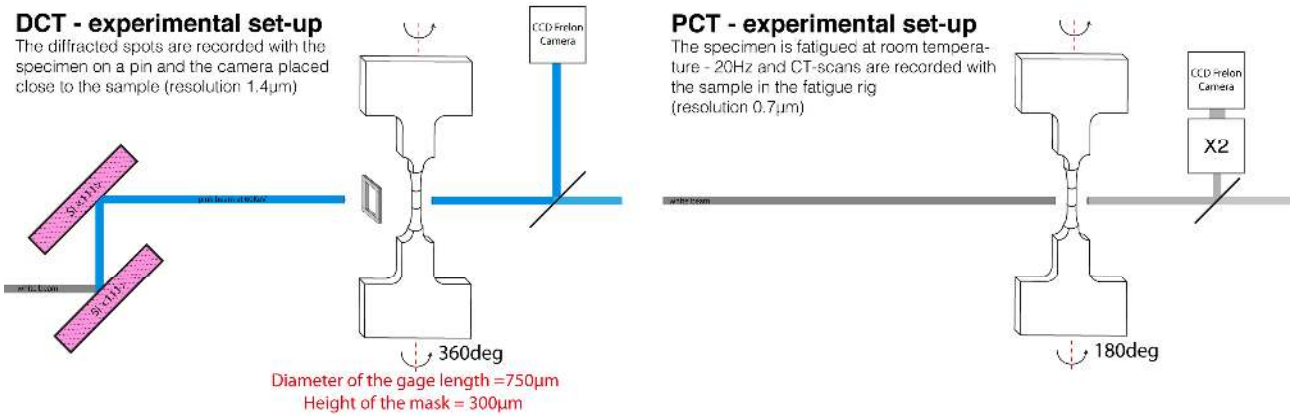

Figure 1: European Synchrotron Radiation Facility (ESRF) setup.

European Synchrotron Radiation Facility Setup

Due to the high attenuation of nickel, the experiment was carried out at ID11 using a high-energy beam (60 KeV) to allow transmission through a representative volume. The Diffraction Contrast Tomography was performed using a 'Pink Beam' (single wavelength), whilst the PCT was carried out using a white beam in order to maximize transmission and improve the definition of the crack. The resolution of the voxel achieved using the DCT is (1.4µm) whilst the resolution of the voxel is improved by a factor of two for PCT through the addition of a lens.

The Diffraction Contrast Tomography was carried out first, with the specimen rotated on a pin. Diffraction images were recorded every 0.05º over the full 360º. The specimen was then placed in the fatigue rig in the same orientation. In the PCT setup, the detector was placed as close as possible to the specimen to inhibit somewhat the phase contrast due to the presence of the crack and thus facilitate its definition. The specimen was fatigued at room temperature under sinusoidal waveform at 20 Hz and R~0.1 with a maximum load equal to 830 MPa (below yield) (details on the machine see [5]). The fatigue experiment was stopped at regular intervals to acquire two orthogonal images to evaluate the crack growth. If significant growth was observed a CT scan was captured (every 0.09º over 180º under 80% maximum load). The specimen investigated, fractured after 200k cycles.

Volume reconstruction for PCT and DCT

The phase and diffraction contrast volume reconstruction has been carried out using an Octave® program from ID19 and a Matlab® program developed in-house on ID11 of the ESRF. For more detailed information regarding the volume reconstruction, please refer to the following publications [6-8]. The DCT volume captured in the vicinity of the crack comprises of more than 5000 grains (including twinned grains).

Defining the crack geometry

The volume processing, meshing, triangulation and visualisation described in this section have been written by the authors and executed in Matlab® 2013a. To follow the crack propagation from the notch, a 3D rigid body translation was performed to align each successive volume scanned to the final volume using immobile features such as pores and the specimen edges. To quicken the analysis the volumes were constrained to that of the crack (*i.e.* last scan at 195k).

Various steps were implemented to detect and enhance the crack definition from the raw dataset. Different thresholding methods were performed on each volume to detect all the features present in the volumes. To differentiate the voxels associated with the crack from those associated with discrete pores, a graph theory 'breadth-first' search was performed. In places, the crack branches, resulting in two overlapping surfaces, which cannot be computed easily. To resolve this, the surface exhibiting the lower values, hence the most open, was selected as the primary crack while the other was saved, meshed and triangulated independently.

In order to produce a realistic crack, interpolated voxels were added to the crack(s) prior to meshing. For each voxel detected as part of the crack, an array was taken along the z-axis, and fitted to a Gaussian envelope; we assumed that the image contrast follows a probability density function, however where the fit did not converge *e.g.*, where the voxel value was just above the threshold value or if the opening is very small; the min. and max values become equal to the mean, *i.e.* the crack opening is null.

A triangular mesh was applied to the resulting surface using Delaunay triangulation and the contour constrained via traveling salesman approach performed on the edge voxels. Finally, to aid the visualisation of the crack surface orientation, the normal to each triangle was linked to a legend coloured according to orientation (Figure 4a).

Post-Mortem Analysis

Electron Backscattered Diffraction (EBSD) map has been acquired post-mortem to corroborate the results obtained using the DCT volume. The electropolished surface and the limited deformation allowed the use of EBSD without additional treatment.

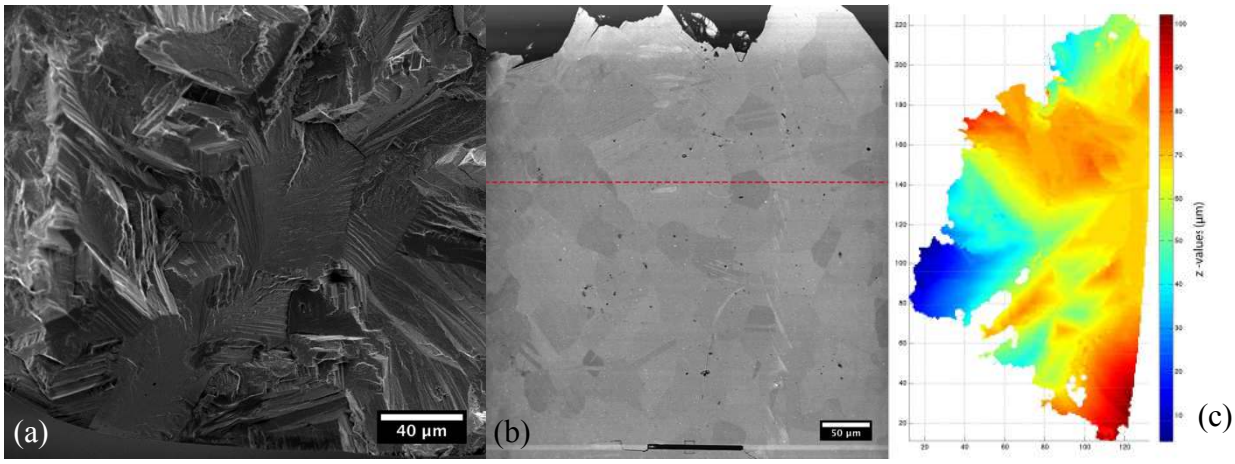

Figure 2: (a) Secondary electron image of the primary crack surface, exhibiting large facets. (b) Backscattered electron image showing the crack profile. The dashed red line shows the upper limit of the PCT volume acquired (notch visible at the bottom of the image). (c) Crack surface at 190k, with colour associated with the z value of the crack position; (scales x, y, z are given in µm).

Results

As shown in Figure 2b, the crack did not fail from the notch towards the bottom of the figure, but from another location outside of the field of view. The primary crack (Figure 2a) initiated from the surface close to a twin boundary in a favorably oriented grain and exhibits a large facet on the fracture surface. The grain orientation maps (EBSD and DCT) show that the secondary crack at the notch intersects multiple grains, which made it particularly difficult for a crack to initiate and propagate (Figure 3) despite the stress concentration at the root.

The fatigue crack front was extracted as described for all the PCT volumes recorded. Figure 4b shows the projection of the heavily serrated crack fronts. These serrations could be artifacts where the crack is accurately closed during scanning. Clearly, where the crack has reclosed no absorption contrast will be visible, although some phase contrast will be apparent giving a different image profile.

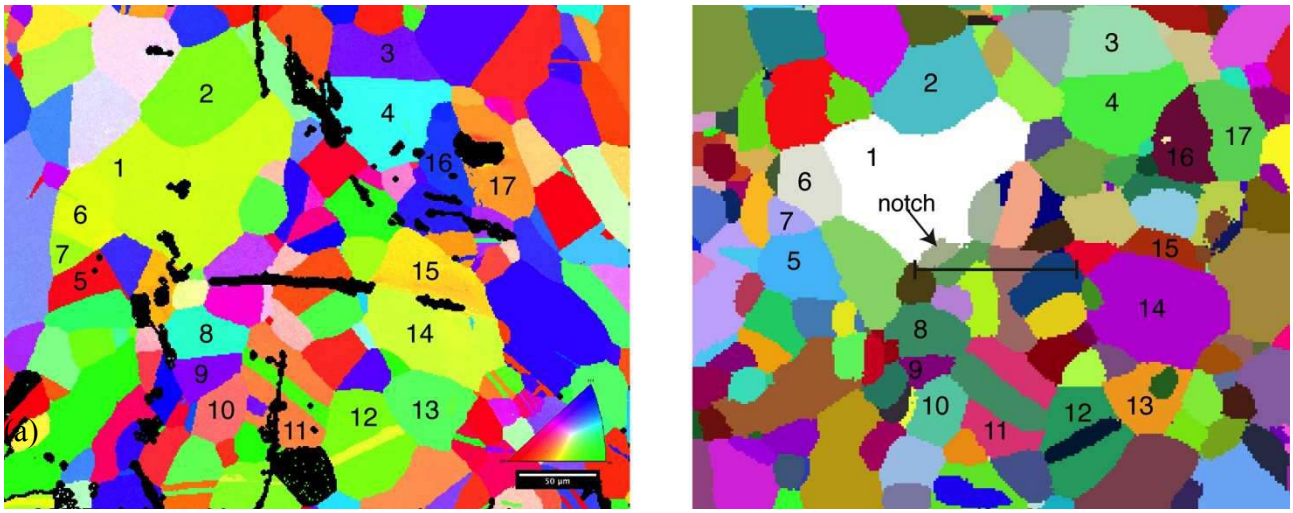

Figure 3: (a) EBSD map collected post-mortem (Inverse Pole Figure-Y), the black region corresponds to unindexed points and (b) Map constructed from DCT data, using random colour, note the notch is not apparent in this dataset, but has been place for reference. Some of the grains have been numbered to highlight the correlation between EBSD map and DCT volume

The closure occurred because the secondary crack (imaged) was shielded by the primary crack from the 80% maximum tensile stress imposed during the scan. Examples where the fracture surface is composed of clean planar facets can be seen labeled in Figure 6c,f. Closure resulted in the crack at 195k cycles (dark red) presenting a slightly smaller area than that at 190k cycles. Additionally, the spikes, A and B visible for 80k and 90k in Figure 4b are associated with the phase contrast from the notch.

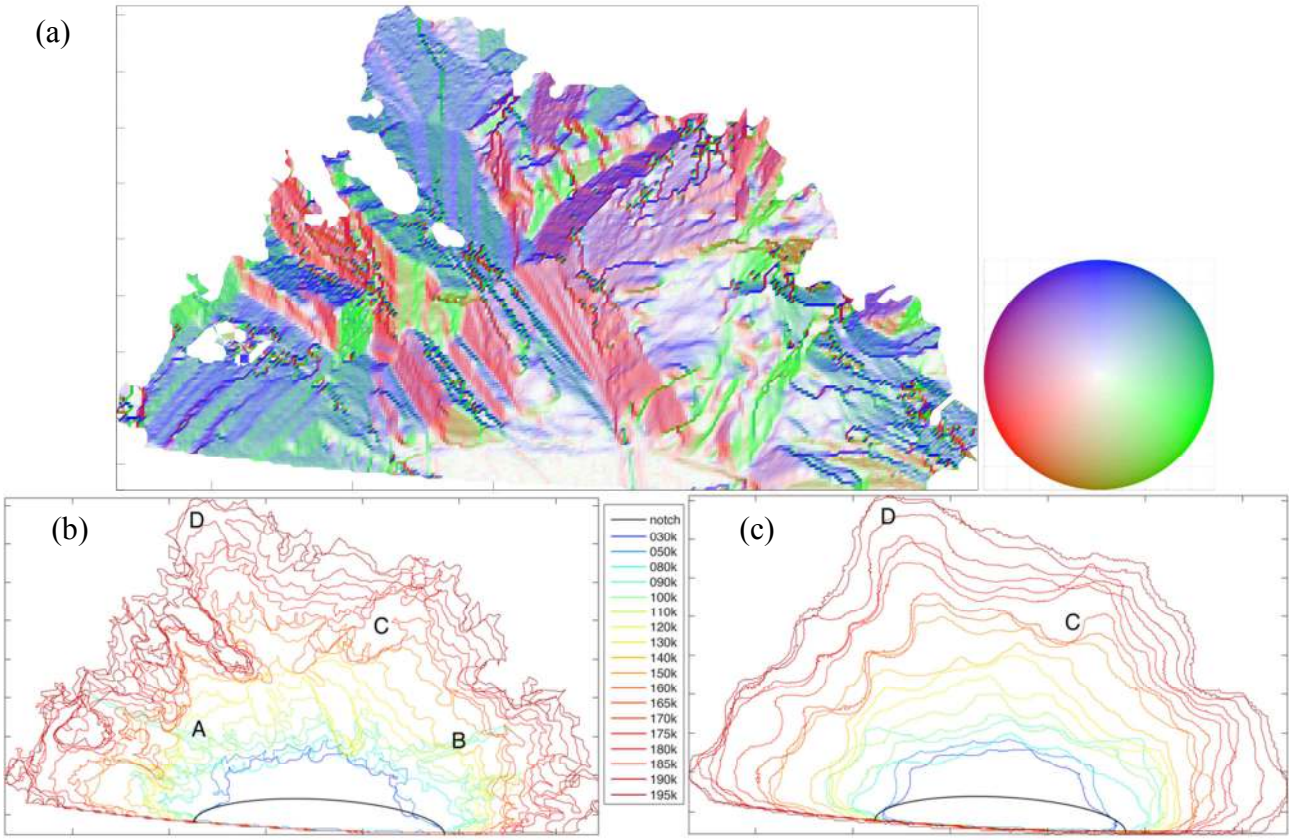

Figure 4. (a) Crack coloured as a function of surface normal orientation at 190k (b) Projected crack front as function of cycles [0-200k:blue-red]. (c) Crack front projection using Chan-Vese segmentation, in black the original notch

To obtain a better idea of the propagation of the crack front over time, Chan-Vese Segmentation (Figure 4c) was used to reduce the constraints on the crack edge. This shows that although the crack

follows an approximately elliptical form, it does not propagate linearly through the material and is sensitive to microstructure and grain orientation. Using this process, the spikes (Figure 4c – A and B) are removed from the crack front (Figure 4c).

The DCT volume size was increased by a factor of two to match the PCT volumes reconstructed. The x and y positions can be aligned from the cross-sections of the two datasets. The EBSD map collected post-mortem and the DCT map show a very good match in both grain shape and position (Figure 3-6). The notch location in the EBSD dataset also provides an accurate location to perform a translation between the datasets along the z-axis. This total affine translation was applied to all volumes and the grain boundary positions are marked in Figure 4a.

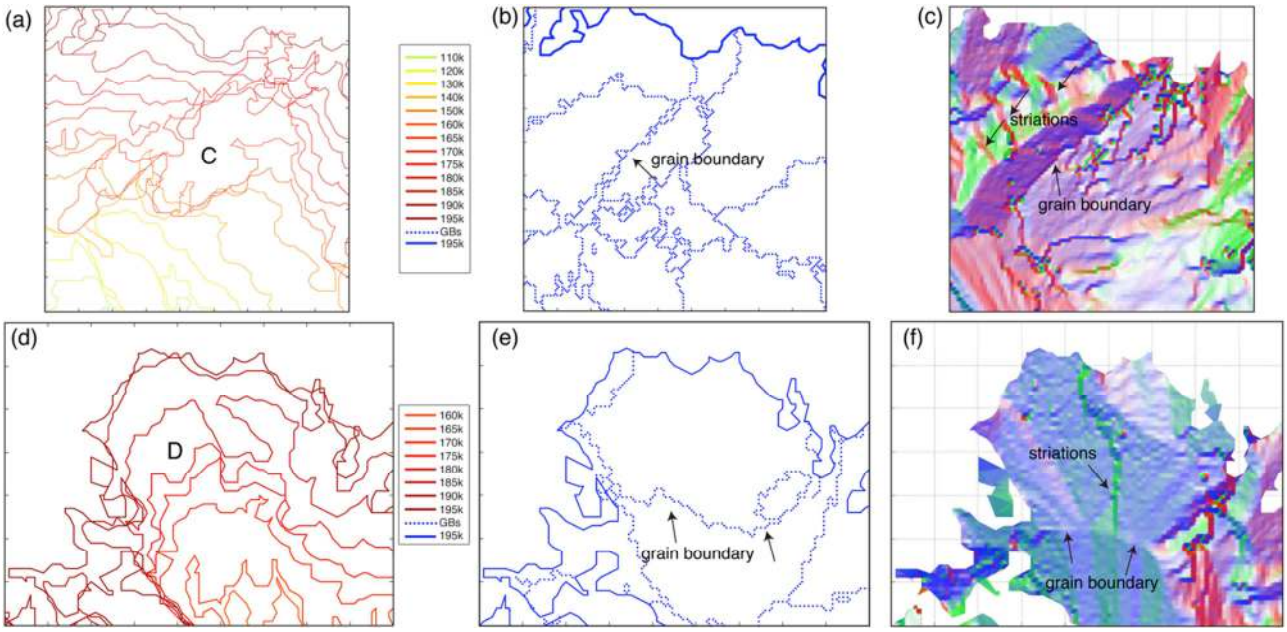

Figure 6: Details from Figure 5 (area C and D) where the fatigue crack propagation front is presented alongside a grain map and surface normal. The first row of images shows a clear interaction between the crack front and grain boundaries. In the second row, the interaction is as evident by the change in crack propagation angle (Figure f), but also illustrates the relatively good fit between the PCT and DCT volumes (please refer to figure 4a for the legend of the figure 6c,f).

Discussion

The fact that the primary crack did not form from the notch is unusual. In trial runs prior to the experiment described here the primary crack developed most often from the notch. Nevertheless the morphology of the two cracks is very similar and characterised by intragranular surfaces, some very planar, others sharply facetted. Propagation is rarely normal to the tensile axis and the crack presents an overall height range in excess of 100 μm, equal to the notch length. Features are closely linked to the grain structure; however, the grain boundaries obtained from the DCT volume do not always exactly match the observed sharp changes in crack plane. This is due to inaccuracies in determining the boundary positions in the DCT volume, but also in aligning the grain structure with the undulating crack position. Work is in progress to improve the accuracy of this.

The observed crack generally grows in a roughly elliptical fashion deepening before widening, as the stress concentration would predict. However the propagation of the crack is not linear over the full surface. One region where the crack is impeded is shown in detail in Figure 6a-c. In this case, the crack remains stationary at position C, during four successive scans amounting to 25k fatigue cycles. This stationary point is located at multiple grain boundaries, but once the crack penetrates through, it results in extremely rapid growth. In the grain above the annotated grain boundary (Figure 6b), the crack surface presents two distinctive planes within the same grain (Figure 6b-c) with the addition of smaller striations; both of these facets are active simultaneously,

and the direction of propagation is parallel to the 'valley'. At the position D (Figure 6d-f), despite the presence of grain boundary, the crack propagation appeared to be mainly unaffected but a change of the propagating plane is evident. This is most likely to minimise the energy required while still accounting for the grain orientation. Work is in progress to relate the crack growth to features of the grains, and also critically, the nature of the boundaries it needs to propagate across.

Conclusions

For the first time a combination of Diffraction Contrast Tomography and Phase Contrast Tomography has been used to follow crack propagation in-situ in a nickel-based superalloy. We have imaged the crack front and related progress through the microstructure, highlighting the sensitivity to the grain arrangement and orientation.

Acknowledgments

The author would like to acknowledge the EPSRC, Grant number EP/H022309/1, EP/H500375/1 and Rolls-Royce plc. under the TSB project 'Siloet' TP NUMBER: AB266C/4 for funding and the Prof Lindsay Greer of the Department of Materials Science and Metallurgy, University of Cambridge for provision of facilities.

References

[1] M.D. Sangid, H.J. Maier, and H. Sehitoglu. An energy-based microstructure model to account for fatigue scatter in polyscrystals. Journal of the Mechanics and Physics of Solids, 59:595–609, 2011.

[2] M.D. Sangid, H.J. Maier, and H. Sehitoglu. The role of grain boundaries on fatigue crack initiation – An energy approach. International Journal of Plasticity, 2010.

[3] J. Miao, T.M. Pollock, and J. Wayne Jones. Crystallographic Fatigue crack initiation in nickel-based superalloy René 88DT at elevated temperature. Acta Materialia, 57(20):5964–5974, 2009.

[4] A.J. Manning, D. Knowles, and C.J. Small. Nickel based superalloy. Patent US 2002/0041821 A1, United States Patent, 2002.

[5] J. Lachambre, A. Weck, J. Réthoré, J-Y. Buffière, J. Adrien. 3D Analysis of a Fatigue Crack in Cast Iron Using Digital Volume Correlation of X-ray Tomographic Images. Imaging Methods for Novel Materials and Challenging Applications, Volume 3, Conference Proceedings of the Society for Experimental Mechanics Series, 203-209, 2013

[6] E. Ferrié, J.-Y. Buffière, and W. Ludwig. 3D Characterisation of the nucleation of a short fatigue crack at a pore in a cast Al alloy using high resolution synchrotron microtomography. International Journal of Fatigue, 27(10-12):1215–1220, 2005

[7] M. Herbig, A. King, P. Reischig, H. Proudhon, E.M. Lauridsen, J. Marrow, J.Y. Buffiere, and W. Ludwig. 3-D growth of a short fatigue crack within a polycrystalline microstructure studied using combined diffraction and phase-contrast X-ray tomography. Acta Materialia, 59:590–601, 2011.

[8] S. Birosca, J.Y. Buffière, M. Karadge, and M. Preuss. 3-D observations of short fatigue crack interaction with lamellar and duplex microstructures in a two-phase titanium alloy. Acta Materialia, 59:1510–1522, 2011.